

Mechanical characterization, Fabrication,

## Experimental determination for Interlaminar tensile strength of reinforced Epoxy composites with Flax fibers for L-angle specimens.

David Pueyo<sup>a\*</sup>, Jesús Cuartero<sup>a</sup> David Ranz<sup>b</sup>, Marcin Barburski<sup>c</sup>

<sup>a</sup> Departamento de Ingeniería Mecánica, Universidad de Zaragoza, Zaragoza, Spain

<sup>b</sup> Departamento de Diseño y Fabricación, Universidad de Zaragoza, Zaragoza, Spain

<sup>c</sup> Institute of Architecture of Textiles, Lodz University of Technology, Lodz, Poland

### *Abstract*

The growing demand of laminated composites materials made of natural fibers and resins with a lower environmental impact in different applications requires a more detailed understanding about the performance during its service considering the delamination in curved parts are one of the most critical failure mechanisms.

The present article pursues to establish a complete protocol to identify the out-of-plane tensile strength of specimens of reinforced unidirectional Epoxy composites with Flax fibers for L-angle specimens using the four-point-bending test in compliance with the ASTM D6415 to determine the interlaminar tensile for a variable thickness.

Several sets of flat specimens and L-shaped unidirectional coupons of Epoxy composites with Flax fibers were manufactured using, liquid resin infusion processing technique (LRI), to determine the mechanical characterization of the composite material and carry out the four-point-bending test. The applicable formulation and the test procedure for the reinforced unidirectional Epoxy composites with Flax fibers on the curved beams with different thicknesses are presented and analyzed.

It was identified the moment of failure when the delamination of the curved beams Flax Epoxy is triggered to calculate The Curved Beam Strength (CBS). Subsequently it was determined the Interlaminar Tensile Strength (ILTS) which is equivalent to the Out-of-plane stress or to the radial stress when reaches the maximum value.

The results obtained for Flax/Epoxy curve beams were analyzed including the post-failure behavior and the evolution of the delamination for maximum interlaminar tensile stress. The extracted conclusions out of the complete process of study provides an understanding of Flax/Epoxy curved beams predictive failure behaviors and the limitations of this material due to the low range mechanical properties results.

### Keywords

Flax Epoxy, Out of the plane stress, Curved Beam Strength, Interlaminar tensile strength, Delamination, Four-point-bending.

## 1. Introduction.

There is an enhanced interest to keep developing more sustainable materials; among them stands out the natural fibre composites due to their versatility and their potential to reduce environmental degradation, which are being introduced as a feasible alternative to traditional materials over a wide range of applications [1]. Even if the focus is on the fibre composites and the creation of fully recyclable structure it is at the early stages, there are already areas where it is proved there is a significant impact. While different natural fibres (flax, hemp, jute and kenaf) carbon footprints are slightly different, it is found those are considerably lower when we compare them to their counterparts as glass and mineral fibres, i.e. The production of 1 ton of natural fibres shows a carbon footprint of about 80% lower than that of glass fibres (until the factory gate, excluding transport to the customer, using mass allocation) [2].

Even if using flax to reinforce polymers is not a new idea, in 1939 De Bruyne et al. [3] already introduced these materials for aviation applications, for the past two decades broad research has been performed. Flax fibres is one of the most popular natural sources of materials reinforcement, reinforce Epoxy composites with Flax fibers applications are being defined progressively while new studies keep providing information about the material characterization and performance.

Application in complex geometries where the components are subjected to wide range thorough-the-thickness loadings which are mainly supported by shapes with high bending radii represent one of the most important challenges. In most of the cases the main mechanism of failure for this type of components comes from the out of plane stresses arisen by the applied moment which will result into Interlaminar Tensile Strength (ILST) leading to interlayer delamination [4,5].

The design of the structure could be effectively performed thorough an accurate estimation of the onset of delamination, which can be done using different criteria of failure [6-8]. However, the higher criticality for these structures is related to the identification of the out of plane tensile strength which is essential for determining the Interlaminar Tensile Strength (ILST); defined as the maximum radial stress or the ordinary interlaminar stress either in the moment of failure or when delamination begins, both equivalent moments.

This study pursues to experimentally evaluate how Interlaminar Tensile Strength (ILTS) evolves for different stacking sequences resulting variable laminated thickness, using four L-angle unidirectional flax/epoxy test coupons with 6,12,18,22 plies.

The ILTS can be calculated using several methodologies, which could be divided into numerical, direct and indirect methodologies. Prediction of ILTS by numerical procedures has been approached by Raju [4], by Avalon [9] and Ross [10]. ASTM C297 [11] and ASTM D7291 [12] are direct load methodologies applying out of plane uniaxial tensile loading to waisted specimens. Although the direct test methodologies are mostly simple to perform there are downsides to be considered. This type of coupons are relatively difficult to manufacture, stress concentrations can anticipate failure near the edges which produce delamination at the free edges [13], in order to avoid such effect direct methods are usually limited to very thick samples to achieve the uniaxial stress in the gauge section preventing early failure due to stress concentrations in the area close to the edge [14-17], and the analysis can be very complex due to the need for an accurate description of the edge effects [18,19], and the tensile stress can only be done for few stacking sequences which is not representative for the general purpose of this study.

Indirect experimental methods are exposed by Makeev [20], Martin [21], Roos [10], and Ko [22] and a comparative analysis about performance of them, including benefits and cons, were presented by Vanttinen [23] and Hara [24].

The four point bending test which was proposed initially by Jackson [25], presents an acceptable complexity of the associated analysis methodology and also moderate experimental difficulties related to the manufacturing of the coupons and the mechanical test. As consequence this test has been standardized, in accordance with ASTM D6415 [26], being the one selected for the ILTS study in this article.

The present article pursues to establish a complete protocol to identify the out-of-plane tensile strength of specimens of reinforced unidirectional Epoxy composites with Flax fibers for L-angle specimens using the four-point-bending test in compliance with the ASTM D6415 [26] to determine the interlaminar tensile for a variable thickness.

This indirect methodology has various advantages over other indirect methods, i.e., stress is irrespective of angular position, the coupon is self-aligned, the bending moment in the tested section is constant and resulting in lower complexity methodology calculation of the ILTS [27]. In addition, it is a more realistic approach to determining interlaminar tensile strength for many applications with a curved geometry, and authors such as Cui [5] or Jackson [25] in their research validate the use of curved beams under four point bending so as to obtain interlaminar tensile strength values. On the other hand, there are some disadvantages mainly the ones for specimens with low bending stiffness, or high values of interlaminar strength having excessive bending of the specimen legs.

## 2. Materials and methods

### 2.1. Materials

Non-crimp unidirectional flax fabric with fibres oriented at 0° and density  $\rho = 280 \text{ g/m}^2$  suitable for manufacturing fibre reinforced composite products with high performance and low environmental impact was utilized to reinforce a polymer composite material, while epoxy resin which has 35% of its molecular structure coming from plant origin was utilized as matrix.

The mechanical characteristics of the Flax Fibre and Epoxy resin used are given in the *Table 1* and *Table 2* respectively.

#### Technical specifications Dry fibres

|         |                                | Value | Units |          |                                | Value | Units |
|---------|--------------------------------|-------|-------|----------|--------------------------------|-------|-------|
| Tension | Tension Modulus // to fibres   | 61    | Gpa   | Flexural | Modulus // to fibres           | 57    | Gpa   |
|         | Modulus ⊥ to fibres            | 6.4   | Gpa   |          | Modulus ⊥ to fibres            | 6.3   | Gpa   |
|         | Strength // to fibres          | 580   | MPa   |          | Strain to failure // to fibres | 663   | MPa   |
|         | Strength ⊥ to fibres           | -     |       |          | Strength ⊥ to fibres           | -     |       |
|         | Strain to failure // to fibres | 1%    |       |          | Yield strength // to fibres    | 348   | MPa   |
|         | Strain to failure ⊥ to fibres  | -     |       |          | Density                        | 1350  | kg/m3 |

\* Composite properties measured on samples (54% fiber volume), with Epoxy resin Araldite LY 8615/ XB 5173

Table 1. Mechanical characteristics of the Unidirectional 0° Flax Dry Fibres

#### Mechanical Properties Of Pure Resin

| Type                          |                        | GP33/SD 4772                  |                        |                               |                      |
|-------------------------------|------------------------|-------------------------------|------------------------|-------------------------------|----------------------|
| Cure                          |                        | Ambient + 24 hrs 40 °C        |                        |                               |                      |
| <b>Tension</b>                |                        | <b>Flexion</b>                |                        | <b>Charpy impact strength</b> |                      |
| Modulus of elasticity         | 3200 N/mm <sup>2</sup> | Modulus of elasticity         | 3300 N/mm <sup>2</sup> | Resilience                    | 18 KJ/m <sup>2</sup> |
| Maximum resistance            | 56 N/mm <sup>2</sup>   | Maximum resistance            | 100 N/mm <sup>2</sup>  | <b>Glass Transition</b>       |                      |
| Resistance at break           | 56                     | Elongation at max. resistance | 3.7 %                  | DSC – TG1 Onset               | 67 °C                |
| Elongation at max. resistance | 1 %                    | <b>Compression</b>            |                        | DSC – TG1 Onset max           | °C                   |
| Elongation at break           | 1 %                    | Compression yield strength    | 110 N/mm <sup>2</sup>  |                               |                      |
| <b>Shear strength</b>         | 51 N/mm <sup>2</sup>   | Offset compression yield      | 9.0 %                  |                               |                      |

Table 2. Mechanical characteristics of the Epoxy Resin (with hardener) without reinforcing

## 2.2. Mechanical Properties

It is required the mechanical characterization of the composite material which will provide the mechanical properties values to obtain the interlaminar Tensile Strength (ILTS). Initially, three laminated composite boards specimens were manufactured by applying a liquid resin infusion processing technique (LRI), *Figure 1* shows the fabrication process applied for manufacturing the composite specimens. Vacuum assisted RTM (Resin Transfer Moulding) system was designed for resin injection into a flat 270 mm by 250 mm mould, staking 6 layers of flax fibre for each one of the three boards, one using fibres oriented at 0°, second one with fibres oriented at 90°, and the third one with fibres oriented at 45°. With the RTM system the dry fibre cuts were included between airtight moulds and subsequently resin/hardener was injected from one side, ensuring an evenly distributed resin/hardener combination without air bubbles by mean of vacuuming with a negative pressure gradient of 620 mmHG. The resulting composite boards have a mixture ratio of resin+hardener 52% and fibre 48%. After the injection process, the moulds were heated by electric oven for curing. Polymerization was completed for 24 h at 40 °C. The resulting thickness for each one of the three composite boards were approximately 3 mm.

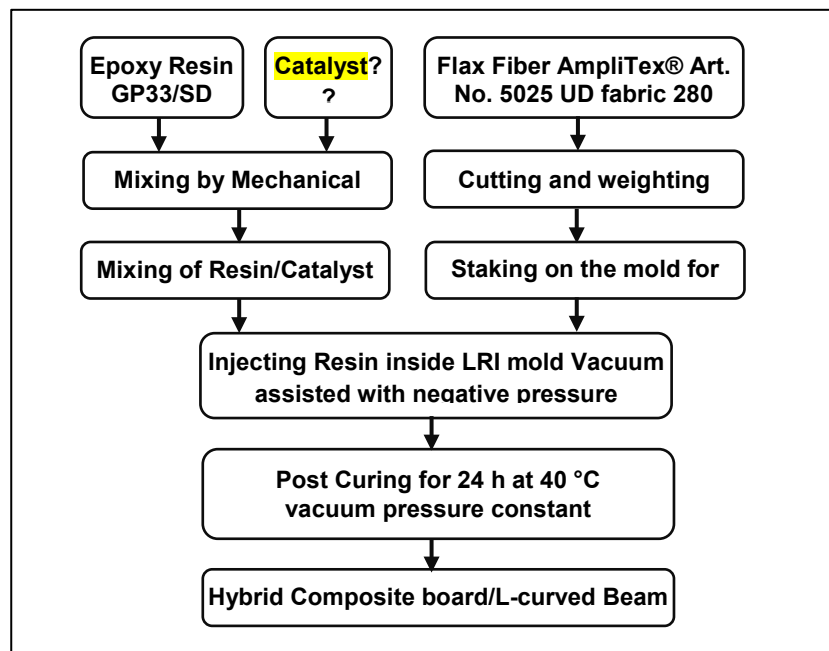


Figure 1. Process Flow Chart Fabrication for Flax-Epoxy composite specimens

After the curing process, the plates made were cut in a total of 10 specimens which were extracted of each board to obtain rectangular shaped specimens for tensile test according to [28] and according to [29] for shear test. The cross-sections for each specimen were measured and recorded before the test. Tensile test and shear test were performed, and the experimental data obtained were statistically processed to determine the mechanical properties, the average values are summarized in the *Table 3*.

### Tests results 0°

|         | Width (a) | Thickness (e) | Tensile Load (F) | Tensile Strength ( $\sigma_{xt}$ ) | Tensile Modulus ( $E_{xt}$ ) | Failure Elongation ( $\epsilon_{xt}$ ) | Poisson Coefficient ( $\nu_{xy}$ ) |
|---------|-----------|---------------|------------------|------------------------------------|------------------------------|--|------------------------------------|
|         | mm        | mm            | kN               | MPa                                | GPa                          | strain (%)                             |                                    |
| Average | 25.83     | 2.93          | 10.61            | 140.13                             | 12.82                        | 1.45                                   | 0.33                               |

### Tests results 90°

|         | Width (a) | Thickness (e) | Tensile Load (F) | Tensile Strength ( $\sigma_{xt}$ ) | Tensile Modulus ( $E_{xt}$ ) | Failure Elongation ( $\epsilon_{xt}$ ) |
|---------|-----------|---------------|------------------|------------------------------------|------------------------------|--|
|         | mm        | mm            | kN               | MPa                                | GPa                          | strain (%)                             |
| Average | 25.80     | 2.58          | 1.12             | 16.72                              | 3.15                         | 0.57                                   |

### Tests results Cortadura 45°

|         | Width (a) | Thickness (e) | Tensile Load (F) | In plane shear Strength ( $\sigma_{yc}$ ) | In plane shear Modulus ( $E_{yc}$ ) | Maximum Shear Elongation ( $\epsilon_{yc}$ ) |
|---------|-----------|---------------|------------------|---|-------------------------------------|--|
|         | mm        | mm            | kN               | MPa                                       | GPa                                 | strain (%)                                   |
| Average | 25.89     | 3.05          | 4.59             | 29.08                                     | 4.68                                | 2.52   |

Table 3. Values Mechanical Properties Tensile and Shear test for Flax/Epoxy coupons

## 2.3 Design and manufacturing of the L angle specimens

Four laminated composite specimens L-boards were manufactured following the same process introduced in the *Figure 1*. The L specimens were made from unidirectional flax fabric and a curved L-plate was utilized to shape the boards as per the industrial standard ASTM D6415 [26] which provides a detailed description of the design of an L-angle specimen manufactured for unidirectional fabric and for a given thickness.

To evaluate how Interlaminar Tensile Strength (ILTS) evolves for different stacking sequences each one of the L-boards it was manufactured with a different number of layers using 6,12,18,22 plies respectively, the unidirectional flax was oriented towards the specimen laterals and along the curved area as shown in the *Figure 2*. The resulting thickness for each one of the four composite L- boards were different. There is no existing rule for the design of L-angle specimens when different thicknesses or different stacking sequences have to be considered in a test campaign.



Figure 2. Resin Infusion process manufacturing for L-curved coupons of Flax Fabric and Epoxy

The curved L-boards were cut in L-shaped coupons as per the industrial standard ASTM D6415 [26]. Poor material fabrication practices, lack of control of fiber alignment, and damage induced by improper L-board machining are known causes for defective specimens' fabrication. Due to defective manufacturing procedures some authors [5,30,31] have reported the diminution in ILTS value when specimen's thickness increases caused by volumetric effects. Noting the

higher the volume the higher the presence of defects, such as gaps or resin accumulation or residual stresses which may induce delamination.

Other important aspects of the specimen preparation that contribute to data dispersion includes thickness variation, curve geometry, surface roughness, and failure to maintain the dimensions specified in section. Noting the highly sensitive of the approach used for the ILTS calculation to the manufacturing process and the actual fabrication constrains per se of the methodology, special care was applied to follow the dimensional requirements of the standard [26], *Figure 3* It is also important to notice the selected the wide experience accumulated during years with the fabrication methodology selected, which provides a better assurance for a high-quality standardized production.

From each L-board 5 coupons were cut with a width of  $25 \pm 1$  mm wide; It was considered the laminate cross section should have constant thickness and the variation did not exceed 5 % of the nominal thickness for any of the coupons; all the coupons were manufactured within the thickness limits from 2 to 12 mm; the measured inner radius for each one of the coupons was withing  $6.4 \pm 0.2$  mm at the bend; the leg length were of 95 mm. *Table 4* compiles the information with the average dimensions for all the coupons segmented by number of layers.

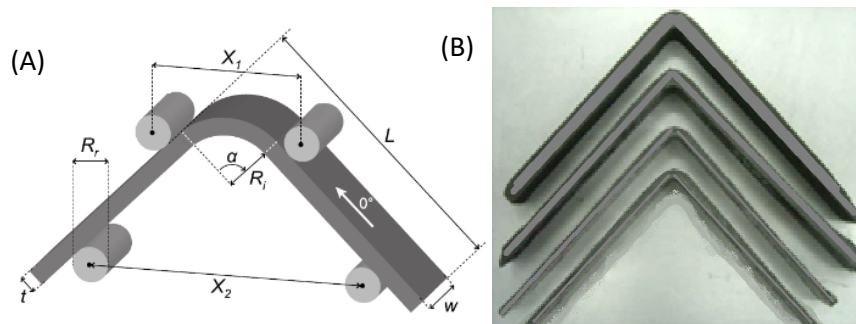


*Figure 3. (A) Configuration of curved L-specimens in four-point test ASTM D6415 [26]; (B) Flax/Epoxy L-shaped coupons for 6, 12, 18 and 22 layers*

***L-Shaped Coupons Dimensional Values***

| <b>Average (mm)</b>  | <b>6 Layers</b> | <b>12 Layers</b> | <b>18 Layers</b> | <b>22 Layers</b> |
|----------------------|-----------------|------------------|------------------|------------------|
| <i>W</i>             | 24.96           | 25.03            | 24.65            | 25.52            |
| <i>L</i>             | 95.65           | 96.05            | 95.39            | 95.73            |
| <i>r<sub>i</sub></i> | 6.48            | 6.46             | 6.43             | 6.44             |
| <i>t</i>             | 3.11            | 6.16             | 8.57             | 11.91            |
| <i>Weight Ratio</i>  | 51%             | 49%              | 51%              | 51%              |

*Table 4. Average values of the Dimensions L-shape Flax/Epoxy Coupons manufactured.*

**2.4 Testing Methodology**

The ASTM D6415 standard is the standardized methodology utilized to define the interlaminar (through-the-thickness) tensile strength (ILTS) in composite materials using L-shape test coupons, where an out-of-plane (through the thickness) tensile stress is produced in the curved region of the specimen to cause the failure [26]. It is specifically defined for interlaminar tensile

strength calculation in curve beams unidirectional fibre layered with all fibres running continuously along the legs and around the bend. Note non-unidirectional specimens may fail due to matrix cracks or free edge stresses which may result in an erroneous interlaminar strength calculation.

The 90° shaped coupon test specimen is used to measure the curved beam strength of a continuous-fibre-reinforced composite material being loaded in four-point bending to apply a constant bending moment across the curved test section, as shown in *Figure 4*. The curved beam strength (CBS) represents the moment per unit width which causes a delamination to form. The four points load on the coupon create a constant bending moment in the curved section tested.

The four-point bending test on L-shape coupons was carried out with an Universal testing machine INSTRON model 8032 (100 KN maximum capability) with the velocity set in controlled displacement mode and a constant displacement rate is imposed of 0.5 mm/min. A fixture manufactured in high strength carbon steel was used to apply the load following requirements of the standard, as shown in *Figure 4*. The fixture has four loading cylinders mounted on roller bearings of 10 mm diameter ( $D$ ); the separation between the top cylinders is 75 mm ( $l_t$ ) and 100 mm ( $l_b$ ) between bottom ones.

The test process for each coupon was recorded with a camera with 108 megapixels definition and he regular and slow-motion recording for 960 fps.

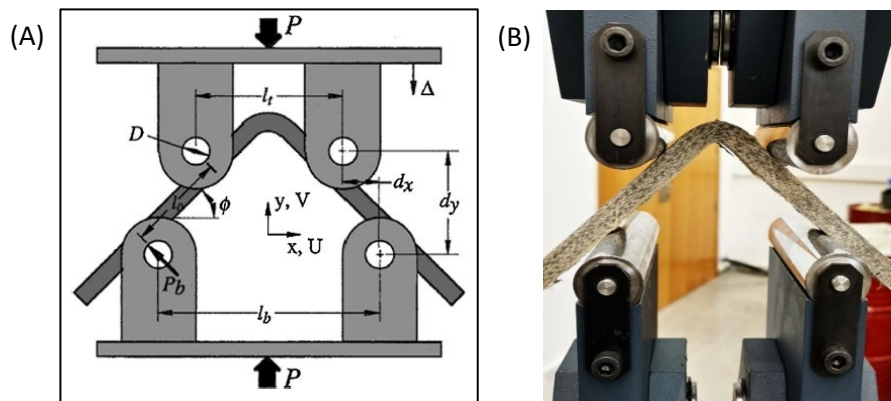


*Figure 4. (A) Diagram for ASTM D6415 Test: [26]; (B) actual experimental device in Universal testing machine INSTRON model 8032*

The four bending points methodology create a complex stress pattern in the curved area of the coupon triggering non-uniform stresses with the critical stress state happening in a small region. The bended area is affected by circumferential compressive stress on the outer surface, by circumferential tensile stresses which are created along the inner surface and by radial tensile stress (out of the plane). The radial tensile stress reaches the maximum peak in the middle third of the thickness (taking as reference the inner surface) and the minimum, zero, at the inner and outer surfaces of the coupon. In this sense, it must be ensured that delamination is triggered to consider the collected data as valid.

## 2.5 Analytical Method

In addition to the testing methodology, the standard ASTM D6415 [26] proposes an analytical method where the data obtained with the four-point bending test on L-angle coupons will provide the frame to calculate the Curved Beam Strength (CBS) and subsequently determine the out of plane normal stress at the failure load (ILTS).

The Curved Beam Strength (CBS) for a L-curved coupon with cylindrical anisotropy can be extracted from the knowledge of the applied loading and of the geometry of the specimen. Considering the 4-point bending test creates a pure bending moment in the coupon curved area, the CBS is determined knowing the actuating moment generated by the force required to trigger the delamination which can be identified due to the abrupt decrease in the load at that moment. Since two forces are applied on each leg of the coupon the loading resultant is null, as a result it can be assumed pure bending for the test section. In addition, the legs need to be considered as a perfectly rigid bodies.

The product of the force applied by one of the cylindrical bars,  $P_b$ , and the distance  $l_o$ , as shown in *Figure 4*, between the upper and bottom cylinder along the leg is the moment applied to the curved section in the specimen, below *Equation 1*. The total force in the first drop determines the strength of the cylinder, and the geometry of the test coupon and the load fixture the distance provides the distance value, below *Equation 1*.

$$CBS = \frac{P_b l_o}{w} = \left( \frac{P}{2w \cos(\phi)} \right) \left( \frac{d_x}{\cos(\phi)} + (D + t) \tan(\phi) \right) \quad (1)$$

$$\text{With } d_y = d_x \tan(\phi_i) + \frac{D+t}{\cos(\phi_i)} - \Delta$$

(1)

$$\text{And } \phi = \text{sen}^{-1} \left( \frac{-d_x(D+t) + d_y \sqrt{d_x^2 + d_y^2 - D^2 - 2Dt - t^2}}{d_x^2 + d_y^2} \right)$$

In the *Equation 1*, to obtain CBS:  $\phi$  stands for the angle in degrees of the loading arm from the horizontal plane,  $P$  is the total applied loading,  $w$  the width of the L-curved coupon,  $U$  the angle in degrees of the leg from the horizontal,  $D$  the diameter of the cylindrical bars,  $t$  the thickness of the tested specimen and  $d_x$  represents the horizontal distance between the centres of the adjacent rollers  $(l_b - l_t)/2$ , *Figure 4*.

Noting that  $\phi$  may change decisively during the loading process, the value of  $\phi$  should be calculated at the failure load, which will allow to determine the value for the calculated moment more accurately. To determine  $\phi$ , firstly, the vertical distance between the loading cylinders needs to be determined,  $d_y$ , which is calculated deducting the vertical displacement,  $\Delta$ , from the initial value of  $d_y$  applied by the test fixture.

To calculate  $d_y$ , is necessary to consider the geometry configuration and the initial angle,  $\phi_i$ . The initial angle is half the global angle between the coupon legs at the initial position prior the test. Finally, using trigonometric functions, a value of  $\phi$  can be determined for a given value of  $d_y$ . Note the rest of the parameters of the equation to calculate  $\phi$  remain with no variation during the entire loading process.

*Equations 2 and 5* were developed by Lekhnitskii [32] and adopted by many other authors [5,25,30] to calculate stresses in a curved beam segment with cylindrical anisotropy from the knowledge of the CBS. At the macroscopic scale, the behavior is assumed linear elastic.

$$\sigma_r = -\frac{CBS}{r_o^2 g} \left[ 1 - \frac{1 - \rho^{\kappa+1}}{1 - \rho^{2\kappa}} \left(\frac{r_m}{r_o}\right)^{\kappa-1} - \frac{1 - \rho^{\kappa-1}}{1 - \rho^{2\kappa}} \rho^{\kappa+1} \left(\frac{r_o}{r_m}\right)^{\kappa+1} \right] \quad (2)$$

$$\sigma_\theta = -\frac{CBS}{r_o^2 g} \left[ 1 - \frac{1 - \rho^{\kappa+1}}{1 - \rho^{2\kappa}} \kappa \left(\frac{r_m}{r_o}\right)^{\kappa-1} + \frac{1 - \rho^{\kappa-1}}{1 - \rho^{2\kappa}} \kappa \rho^{\kappa-1} \left(\frac{r_o}{r_m}\right)^{\kappa+1} \right] \quad (3)$$

$$\tau_{r\theta} = 0 \quad (3)$$

Considering:

$$g = \frac{1 - \rho^2}{2} - \frac{\kappa}{\kappa + 1} \frac{(1 - \rho^{\kappa+1})^2}{1 - \rho^{2\kappa}} + \frac{\kappa \rho^2}{\kappa - 1} \frac{(1 - \rho^{\kappa-1})^2}{1 - \rho^{2\kappa}} \quad (4)$$

$$\kappa = \sqrt{\frac{E_\theta}{E_r}}$$

$$\rho = \frac{r_i}{r_o}$$

$$r_m = \left[ \frac{(1 - \rho^{\kappa-1})(\kappa + 1)(\rho r_o)^{\kappa+1}}{(1 - \rho^{\kappa+1})(\kappa - 1)r_o^{-(\kappa-1)}} \right]^{\frac{1}{2\kappa}} \quad (5)$$

$$\sigma_r^{max} = \frac{3 \cdot CBS}{2t\sqrt{r_i r_o}} \quad (6)$$

For a given laminated plate the moduli in the circumferential direction  $E_\theta$ , is equal to longitudinal moduli  $E_1$ ; while moduli in the radial direction  $E_r$ , is equivalent to transversal moduli,  $E_3$ , respectively.

Once CBS is calculated with the *Equation 1*, it can be determined the Out-of-plane stress or radial stress ( $\sigma_r$ ) when reaches the peak value using the *Equation 2*. Interlaminar Tensile Strength (ILTS) is identified at the moment of failure when the delamination is triggered which is equivalent to the maximum radial stress.

Calculation of the Interlaminar Tensile Strength (ILTS) using the *Equation 4* can be simplified within a 2% error magnitude when the ratio  $E_\theta/E_r$  is lower than 20. ILTS or  $\sigma_r^{max}$ , maximum radial stress approximation can be calculated using the *Equation 6*. Note the accuracy of the results is lower whenever the ratio  $r_i/r_o$  increases and is higher when the  $E_\theta/E_r$  ratio decreases.

### 3. Results and discussion

#### 3.1 Four point bending test Results

A sequence of tests were done for at least 5 L-curved coupons for each thickness sample. This is 6, 12, 18 and 22 unidirectional flax layers, with an average thickness of 3.11, 6.16, 8.57 and 11.91 mm respectively.

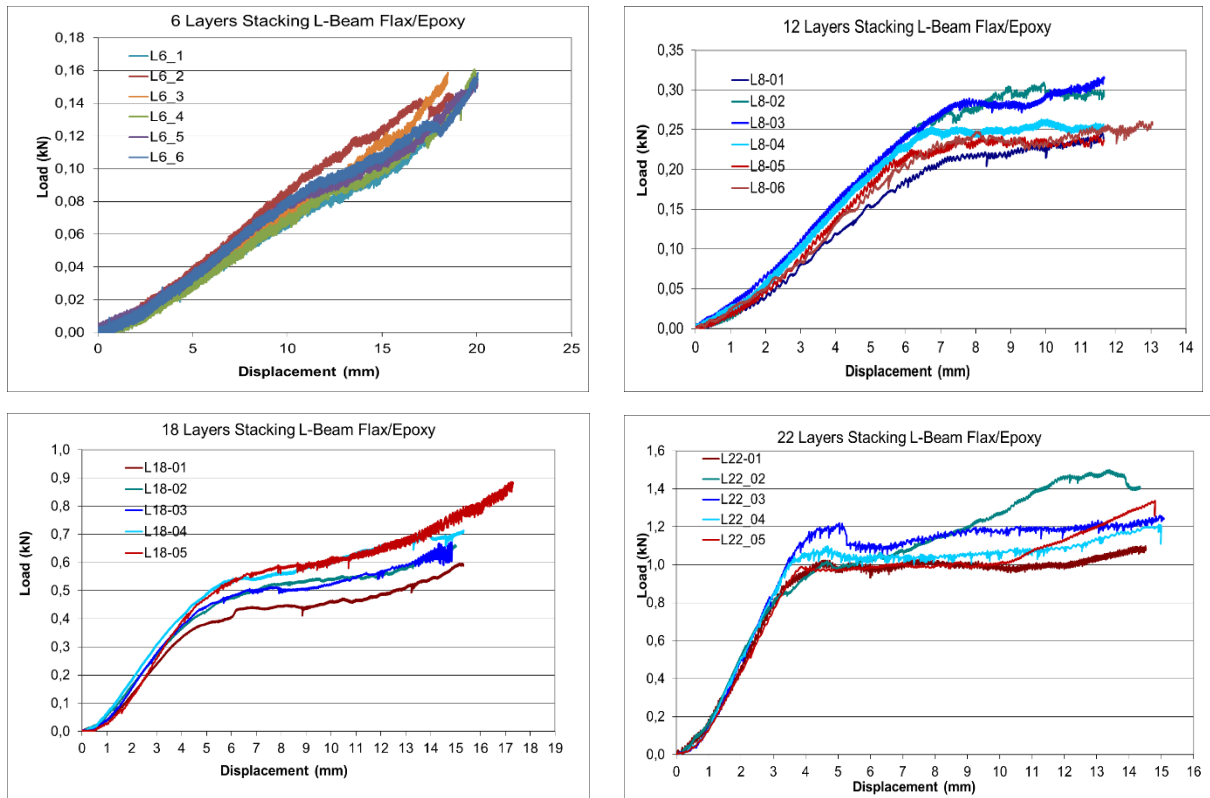


Figure 5 Load Displacement Graphs as for Flax/Epoxy L-shaped coupons with 6,12,18 and 22 layers

Test results can be seen into the *Figure 5* where graphs resulting from the four-point bending test are displayed. As it would be expected, the coupons are behaving elastically as they reach the maximum load admitted for each coupon until the delamination begins. Typically, it would have been expected an abrupt drop in the load when delamination begins and subsequently secondaries recoveries and drops for each additional delamination of other interface. In the graphs The delamination trigger point for the Flax/Epoxy coupons can be identified at the point where there is a load reduction which could be identified in the graph as a slope change from the progressive elastic behaviour.

The test process for each coupon was recorded with a camara with 108 megapixels definition and slow-motion recording for 960 fps. The detailed analysis of the initiation of the crack for the delamination and the graph behaviour confirmed the slope change point, taking as reference the end of linear elastic behaviour, as the point where the initial delamination is triggered. *Figure 6* shows a representation of the Maximum load reached prior delamination generally localized at 1/3 thickness from the inner radius.

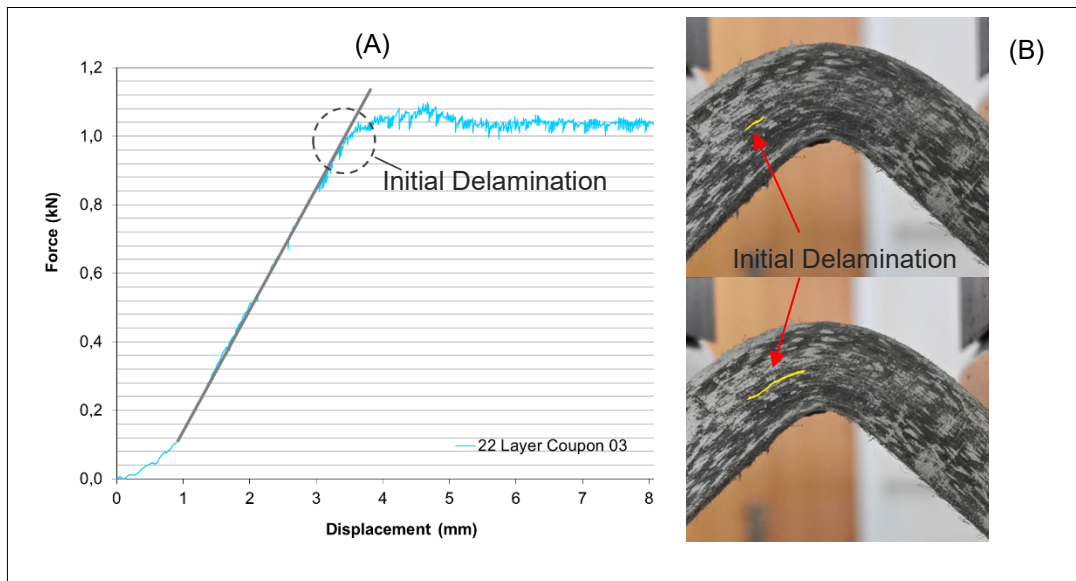


Figure 6. (A) Load Displacement Graph, Maximum Load point prior initial delamination; (B) Coupon initial delamination during four bending point test

The Table 5 compiles the Maximum loads and initial delamination location for each one of the coupons.

#### ***Maximum Load point prior initial delamination***

|                              | <b>6 Layers</b> | <b>12 Layers</b> | <b>18 Layers</b> | <b>22 Layers</b> | <b>Units</b> |
|------------------------------|-----------------|------------------|------------------|------------------|--------------|
| <i>Coupon 1</i>              | 0.081           | 0.188            | 0.36             | 0.886            | <i>KN</i>    |
| <i>Coupon 2</i>              | 0.108           | 0.24             | 0.41             | 0.84             | <i>KN</i>    |
| <i>Coupon 3</i>              | 0.08            | 0.249            | 0.38             | 0.8              | <i>KN</i>    |
| <i>Coupon 4</i>              | 0.09            | 0.225            | 0.45             | 0.85             | <i>KN</i>    |
| <i>Coupon 5</i>              | 0.081           | 0.207            | 0.4              | 0.866            | <i>KN</i>    |
| <i>Coupon 6</i>              | 0.086           | 0.199            |                  |                  | <i>KN</i>    |
| <i>Average</i>               | 0.087           | 0.218            | 0.4              | 0.848            | <i>KN</i>    |
| <i>CV (%)</i>                | 11.87           | 10.91            | 3.79             | 3.79             |              |
| <i>Delamination Location</i> | 2-3             | 3-6              | 4-8              | 5-10             |              |

Table 5. Load at initial delamination failure for Flax/Epoxy L-curved coupons

### **3.2 Determination of Properties and result of analysis**

For each set of coupons which has been segmented by the number of stacking layers, the Curve Beam Strength (CBS), Equation 1 was calculated. For the calculation it has been used the total applied load which in this case is the maximum load admitted prior the delamination and the angle  $\phi$  (Figure 4), between the horizontal plane and the L-curved coupon legs.

The CBS was calculated with two different approaches, first one it would consider the actual variable value of the angle  $\phi$  and the second one would simplify the calculation considering the angle  $\phi$  same as the initial angle,  $\phi_1$  fixed during the test procedure. CBS calculation results are

shown in the *Table 6*, for coupons with 6, 12, 18 and 22 layers. Comparing both calculation approaches, it is noticeable that for 6 layered coupons the variation coefficient shows a reduction of 41,65% of the CBS with no correction versus CBS with actual angle, and a variation of 12,5° in the initial angle  $\phi_i$ . The difference in the results for both methods are considerable, this is because the higher variation of the angle for coupons with low bending stiffness or higher flexibility which results in higher angles on the moment of bending at failure.

For the coupons with 12 layers, 10 layers and 22 layers, there is a variation with respect to the initial angle of 5,36° ,3.58° and 2.67° respectively, which means a CBS reduction of 21.64%, 15.29% and 11.79% in the same order. The higher the number of layers the higher the stiffness and the lower the angle variation, resulting in a lower deviation in the calculation, *Figure 7*. Considering the higher flexibility of the Flax/Epoxy coupons and the results of the sensitivity analysis for both calculation methods, it is recommended to consider the actual variable value of the angle  $\phi$ .

|           | <b>CBS with no correction</b><br>$\phi$ (N·mm/mm) | <b>Angular Deflection</b><br>$\phi$ | <b>CBS</b><br>(N·mm/mm) | <b>CBS Variation Coefficient</b><br>(%) |
|-----------|---|-------------------------------------|-------------------------|---|
| 6 layers  | 185.78  | 12.74                               | 108.48                  | -41.61%                                 |
| 12 layers | 491.30  | 5.36                                | 385.11                  | -21.62%                                 |
| 18 layers | 702.50  | 3.58                                | 595.27                  | -15.26%                                 |
| 22 layers | 1333.11   | 2.56                                | 1181.56                 | -11.37%                                 |

*Table 6. Curve Bean Strength CBS calculation with and without correction.*

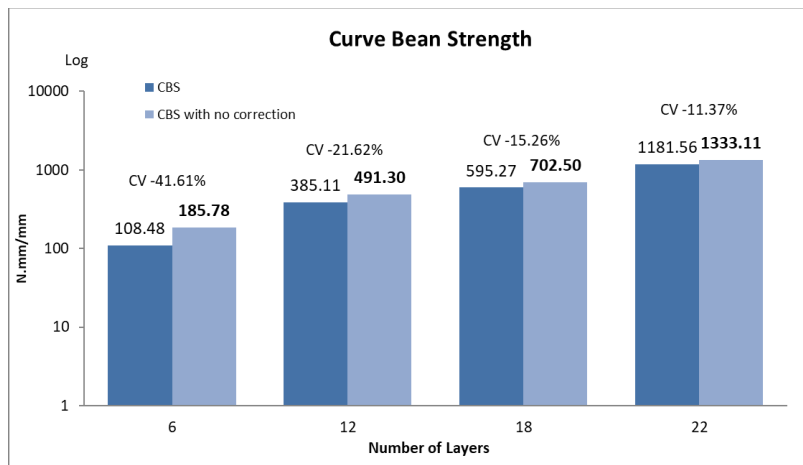


*Figure 7. Sensitivity analysis CBS Variation Coefficient vs. Number of layers for Flax/Epoxy L-shaped coupons*

Three different approaches have been taken to determine the Out-of-plane stress or radial stress ( $\sigma_r$ ) when reaches the maximum value, which is the same as the Interlaminar Tensile Strength (ILTS). First one is calculated with Lekhnitskii formulation [32] using *Equation 2* and (4). For the second approach, knowing the Interlaminar Tensile Strength (ILTS) formulae can be simplified when the ratio  $E_\theta/E_r$  is lower than 20 within a 2% error magnitude the simplified *Equation 6* was utilized and the last approach. For the third methodology same simplified *Equation 6* was applied to determined Interlaminar Tensile Strength (ILTS) including in this case

the CBS value with not correction considering the angle  $\phi$  same as the initial angle,  $\phi_i$  fixed during the test procedure.

For the simplified calculation it is used the mechanical properties calculated in the section 2.2 and the mechanical characterization of the analysed Flax/Epoxy laminate. Also, it is considered the values for the moduli in circumferential direction is equivalent to the longitudinal moduli  $E_\theta = E_1 = 12,82$  GPa and the moduli in radial direction is equivalent to the transversal moduli  $E_r = E_2 = 3,15$  GPa, which leads to have a ratio of  $E_\theta/E_r = 4,07$

In the *Table 7*, it has been included the calculation for the ILTS values segmented by number of layers, both simplified, *Equation 6* and Lekhnitskii [32] formulation, which have been determined as the average of the ILTS calculated for each one of the coupons with the same number of layers. From the observation of the table values, we can extract the following observations:

- ILTS value is lower when Lekhnitskii [32] formulation is used versus the simplified option.
- When the ratio  $r_i/r_o$  ( $\rho$ ) decreases or the ratio  $E_\theta/E_r$  increases the deviation between both methods increases, which means the accuracy of the simplified solution is lower. For the analysed laminates the ratio  $E_\theta/E_r$  has a value of 4,07, which is lower than 20. The calculated error also remains under 2% for all the coupons thickness tested even for the case of the thickest coupon which is the 22 layers the deviation using the simplified formula is 1,91%. These results provide a base to accept the simplified solution as an approximation in those cases where an error lower than 2% can be acceptable.
- The ILTS value calculated for the 6 layers coupon is significantly lower than the rest of the ILTS values for the other stackings. As it is specified into the standard ASTM D6415 [26] specimens with low bending stiffness, may exhibit excessive bending of the specimen legs during flexural loading and can create large errors in the calculated bending moment, resulting in unconservative strength calculations. As discussed in the section 3.2 the variation with respect to the initial angle is  $12,74^\circ$  and we are working with cross head displacements about 10 mm, when the standard indicates if the cross-head displacement exceeds 5 mm prior to failure significant error may occur in the bending moment calculation due to flexure of the specimen legs. Having those arguments into consideration it is noted the deviation of the ILTS for 6 layers is very significant and invalidate the calculation result and procedure for the 6 layers specimens.
- When compared the ILTS values obtained through Lekhnitskii [32] formulation, considered as the more accurate ones, the average values for 12, 18 and 22 layers were 10,32, 10,40 and 10,74 MPa, respectively as it can be shown in *Figure 8*. A slight increase is appreciated in the values when the thickness of the specimens increases, volumetric effects can be considered as neglectable in this case.

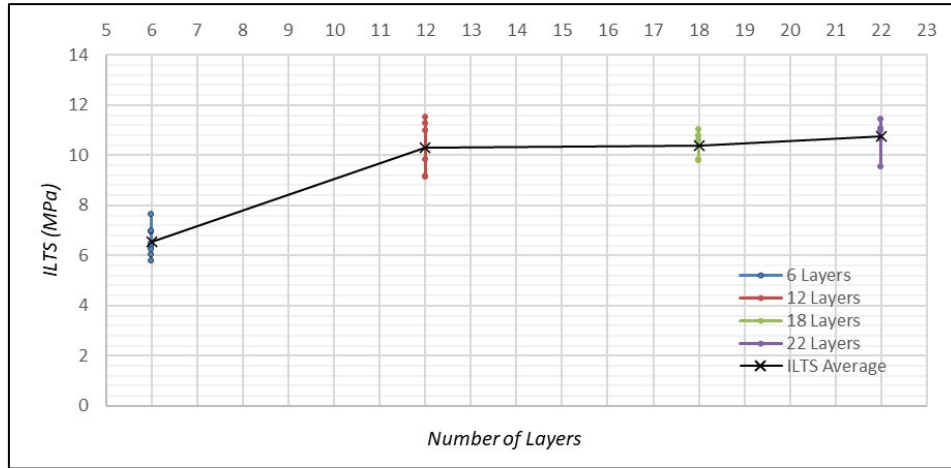


Figure 8. ILTS values segmented by number of Layers in the L-shaped Coupons

|           | <b>Simplified Formulation</b> |               | <b>Lekhnitskii's Formulation</b> |               | <b>Deviation (%)</b> |
|-----------|-------------------------------|---------------|----------------------------------|---------------|----------------------|
|           | <b>ILTS<sub>s</sub> (MPa)</b> | <b>CV (%)</b> | <b>ILTS (MPa)</b>                | <b>CV (%)</b> |                      |
| 6 layers  | 6.59                          | 10.21         | 6.54                             | 10.93         | 0.66%                |
| 12 layers | 10.41                         | 10.46         | 10.32                            | 11.55         | 0.85%                |
| 18 layers | 10.59                         | 5.53          | 10.40                            | 5.50          | 1.74%                |
| 22 layers | 10.95                         | 6.04          | 10.74                            | 6.72          | 1.91%                |

Table 7. ILTS Simplified calculation Vs. ILT from Lekhnitskii's formulation [32].

In the Table 8, it has been included the calculation for the ILTS values segmented by number of layers using two methodologies, the simplified formulation, Equation 6, but also including the CBS values without correction (calculation considering the angle  $\phi$  the same as the initial angle,  $\phi_i$  fixed during the test procedure) and Lekhnitskii [32], both have been determined as the average of the ILTS calculated for each one of the coupons with the same number of layers. Observing the values for the ILTS using the simplified formulation with CBS without correction the highest quantity 13.27 MPa is reached for 12 layers, decreasing for 18 and 22 layers with 12.50 and 12.35 MPa respectively. For 6 layers the value is 11.41 MPa which is the minimum compared to the higher thickness tested coupons. It is also observed that the deviation compared to the Lekhnitskii [32] formulation has a decreasing trend when the specimen thickness increases. Even if there is such trend, the deviation is significant enough and the values not consistent to be considered as reliable, resulting in a not acceptable approximation methodology.

|                  | <i>Simplified Formulation<br/>CBS Not Correction</i> |               | <i>Lekhnitskii's Formulation</i> |               | <i>Deviation (%)</i> |
|------------------|--|---------------|----------------------------------|---------------|----------------------|
|                  | <i>ILTS<sub>s</sub> (MPa)</i>                        | <i>CV (%)</i> | <i>ILTS (MPa)</i>                | <i>CV (%)</i> |                      |
| <i>6 layers</i>  | 11.41  | 15.24         | 6.54                             | 10.93         | 42.64%               |
| <i>12 layers</i> | 13.27  | 11.95         | 10.32                            | 11.55         | 22.28%               |
| <i>18 layers</i> | 12.50  | 5.65          | 10.40                            | 5.50          | 16.74%               |
| <i>22 layers</i> | 12.35  | 6.16          | 10.74                            | 6.72          | 13.08%               |

Table 8. ILTS Simplified Calculation and CBS with not correction Vs. ILT from Lekhnitskii [32 formulation].

#### 4. Conclusions

Flax fibres is one of the most popular natural sources of materials reinforcement. This study has focused the attention to provide a better understanding of the failure of reinforce Epoxy composites with Flax fibers where the components are subjected to wide range thorough-the-thickness loadings which are mainly supported by shapes with high bending radii represent one of the most important challenges, reaching the following conclusions:

It has been established a complete protocol to identify the out-of-plane tensile strength of specimens of reinforced unidirectional Epoxy composites with Flax fibers for L-angle specimens using the four-point-bending test in compliance with the ASTM D6415 [26] to determine the interlaminar tensile for a variable thickness.

Epoxy composites with Flax fibers for L-angle coupons are behaving elastically as they reach the maximum load admitted previously to the delamination begins. For the Flax/Epoxy coupons the delamination trigger can be identified at the point where there is a load reduction is the point where there is a slope change from the progressive elastic behaviour.

The CBS was calculated with two different approaches, first one it would consider the actual variable value of the angle  $\phi$  and the second one would simplify the calculation considering the angle  $\phi$  to the initial angle,  $\phi_i$  fixed during the test procedure. The difference in the results for both methods are considerable, this is because the higher variation of the angle for coupons with low bending stiffness or higher flexibility which results in higher angles on the moment of bending at failure. Although, the higher the number of layers the higher the stiffness and the lower the angle variation, resulting in a lower deviation in the calculation, it is recommended to consider the actual variable value of the angle  $\phi$  for the CBS calculation.

Three different approaches have been taken to determine the Out-of-plane stress or radial stress ( $\sigma_r$ ) when reaches the maximum value which is the Interlaminar Tensile Strength (ILTS). The conclusions considering the results for each one of the approaches are the following:

- ILTS value is lower when Lekhnitskii [32] formulation is used versus the simplified option.
- The calculations has proved the error between the Lekhnitskii [32] formulation and the simplified remains under 2% for all the thickness tested. The simplified solution can be accepted as a reliable approximation for Epoxy composites with Flax fibers in those cases where the tolerance error is 2% or higher..
- The ILTS value calculated for the 6 layers coupon is significantly lower than the rest of the ILTS values for the other stackings which invalidate the calculation results and procedure for ILTS 6 layers specimens. The main reason for this behaviour is coupons with low bending stiffness may exhibit excessive bending of the specimen legs during

flexural loading and can create large errors in the calculated bending moment, resulting in unconservative strength calculations.

- The ILTS values obtained through Lekhnitskii [32] formulation is stable, having a slight increase when the thickness of the specimens increases. Volumetric effects can be considered as neglectable in this case.
- The values calculated using the simplified formulation and also including the CBS values without correction (calculation considering the angle  $\phi$  to the initial angle,  $\phi_i$  fixed during the test procedure) are not consistent and significantly different compared to the Lekhnitskii [32] formulation, as such, the simplified formulation with CBS without correction is not acceptable.

There is a significant difference when we compared the magnitude of the mechanical properties, CBS and ILTS values between the composite used for this study with a base of Flax natural fibres and epoxy versus glass fibre or carbon/epoxy. [33] Those differences indicate using Flax/Epoxy fibres composites in structurally demanding conditions would be very limited.

## References

- [1] Mathijsen Django, «The renaissance of flax fibers,» *Reinforc Plast*; May 2018; 62(3):138-47.
- [2] Niels de Beus, Michael Carus «Carbon Footprint and Sustainability of Different Natural Fibers for Biocomposites and Insulation Material,» European research project MultiHemp (FP7/2007-2013, grant agreement n° 311849), March 2019.
- [3] De Bruyne NA. «Plastic progress. Some further developments in the manufacture and use of synthetic materials for aircraft construction,» *Fligh* 1939;12 January: 77–9.
- [4] D. Raju, «Delamination damage analysis of curved composites subjected to compressive load using cohesive zone modelling,» *QuEST Global*, 2014.
- [5] W. Cui, L. Jianxin y R. Ruo, «Interlaminar tensile strength (ILTS) measurement of woven glass/polyester laminates using four-point curved beam specimen,» *Composites Part A*, vol. 27A, pp. 1097-1105 , 1996.
- [6] Christensen RM, DeTeresa SJ. «Delamination failure investigation for out-of-plane loading in laminates,» *J Compos Mater* 2004;38(24):2231–8.
- [7] Brewer JC, Lagace PA. «Quadratic stress criterion for initiation of delamination,» *J Compos Mater* 1988;22(12):1141–55.
- [8] Kim R, Soni S. «Failure of composite laminates due to combined interlaminar normal and shear stresses,» In: *Proceedings of Japan–US CCM-III*; 1986. p. 341–50.
- [9] S. Avalon y S. Donaldson, «Strength of composite angle brackets with multiple geometries and nanofiber-enhanced resins,» *Journal of Composite Materials*, 2010.
- [10] R. Roos, G. Kress, M. Barbezat y P. Ermanni, «Enhanced model for interlaminar normal stress in singly curved laminates,» *Composite Structures*, vol. 80, p. 327–333, 2007.
- [11] «ASTM C 297-04 - Flatwise Tensile Strength of Sandwich Constructions,» W. Conshohocken, Pa., 1954.
- [12] «ASTM D 7291-07 - Through-Thickness 'Flatwise' Tensile Strength and Elastic Modulus of a Fiber-Reinforced Polymer Matrix Composite Material,» West Conshohocken, PA, 2007.
- [13] O'Brien TK. Characterization of delamination onset and growth in a composite laminate. In: Reifsnider KL, editor. *Damage in composite materials*. ASTM STP775. Philadelphia: ASTM; 1982. p. 140–67.
- [14] Kitching R, Tan A, Abu-Mansour T. The influence of through thickness properties on glass reinforced plastic laminated structures. *Compos Struct* 1984;2(2):105–51.
- [15] Hara E, Yokozeki T, Hatta H, Iwahori Y, Ishikawa T. Comparison of out-of-plane tensile moduli of CFRP laminates obtained by 3-point bending and direct loading tests. *Compos Part A: Appl Sci Manuf* 2014;67:77–85.
- [16] Hodgkinson J, Ayache S, Matthews F. In plane and out-of-plane property measurement on thick woven glass/polyester laminates. In: *ECCM-5, composites testing and standardisation*. Amsterdam, Netherlands: ESCM; 1992.
- [17] Hara E, Yokozeki T, Hatta H, Ishikawa T, Iwahori Y. Effects of geometry and specimen size on out-of-plane tensile strength of aligned CFRP determined by direct tensile method. *Compos Part A: Appl Sci Manuf* 2010;41(10):1425–33.
- [18] Lagunegrand L, Lorriot T, Harry R, Wagnier H, Quenisset JM. Initiation of freeedge delamination in composite laminates. *Compos Sci Technol* 2006;66(10):1315–27.
- [19] Pagano N. Free edge stress fields in composite laminates. *Int J Solids Struct* 1978;14:401–6.
- [20] A. Makeev, P. Carpentier y B. Shonkwiler, «Methods to measure interlaminar tensile modulus of composites,» *Composites: Part A*, vol. 56, p. 256–261, 2014.
- [21] R. Martin, «Delamination failure in an unidirectional curved composite laminate,» National Aeroespacial and Space Administration, Langley Research Center, 1990.
- [22] W. Ko, «Delamination stresses in semicircular laminated composite bars,» Nasa Report, 1988.
- [23] A. Vanttinen, «Strength Prediction of Composite Rib Foot Corner,» Master's Thesis, Helsinki University of Technology, 2008.

- [24] E. Hara, T. Yokozeki y H. Hatta, «Comparison of out-of-plane tensile strengths of aligned CFRP obtained by 3-point bending and direct loading tests,» *Composites: Part A*, nº 43 , p. 1828–1836, 2012.
- [25] W. Jackson y P. Ifju, «Through the thickness tensile stress of textile composites,» NASA. Langley Research Center, 1994.
- [26] «ASTM D6415/D6415M-06a – Standard Test Method for Measuring the Curved Beam Strength of a Fiber-Reinforced Polymer-Matrix Composite,» West Conshohocken, PA, 1999.
- [27] W. Jackson y P. Ifju, «Through the thickness tensile stress of textile composites,» NASA. Langley Research Center, 1994.
- [28] SR EN ISO 14125/2000, Fibre-reinforced plastic composites. Determination of flexural properties.
- [29] SR EN ISO 14129:1997 Fibre-reinforced plastic composites — Determination of the in-plane shear stress/shear strain response
- [30] W. Hao, D. Ge, Y. Ma, X. Yao y Y. Shi, «Experimental investigation on deformation and strength of carbon/epoxy laminated curved beams,» *Polymer Testing*, vol. 31, nº 4, p. 520–526, 2012.
- [31] W. Jackson y R. Martin, «An interlaminar tensile strength specimen,» *Composite Materials: Testing and Design*, vol. 11, pp. 333-354, 1993.
- [32] S. Lekhnitskii, S. Tsai y T. Cheron, «Anisotropic Plates,» Gordon Breach Science Publishers, 1968.
- [33] David Ranz, Jesus Cuartero, Antonio Miravete, Ramón Miralbes, «Experimental research into interlaminar tensile strength of carbon/epoxy laminated curved beams,» *composite Structures*, 2016.